JOINT INSTITUTE FOR AERONAUTICS AND ACOUSTICS

National Aeronautics and
Space Administration
Ames Research Center

JIAA TR - 81

Stanford University

AN ANALYSIS OF CONICAL AUGMENTOR/DELTA WING INTEGRATION

BY

D. A. Tavella, and T. S. Lund

Stanford University
Department of Aeronautics and Astronautics
Stanford, CA 94305

DECEMBER 1987

JIAA TR - 81

AN ANALYSIS OF CONICAL AUGMENTOR/DELTA WING INTEGRATION

BY

D. A. Tavella, and T. S. Lund

Stanford University
Department of Aeronautics and Astronautics
Stanford, CA 94305

DECEMBER 1987

ABSTRACT

The integration of a conical augmentor with a slender conical delta wing is investigated analytically. The study is relevant to the transition phase of VTOL delta wing aircraft, when both aerodynamic lift and propulsive forces due to the augmentors come into play. The analysis is carried out in the cross-flow plane by means of conformal mapping. A conical augmentor gives rise to two main flow fields of relevance to the aerodynamics of a slender delta wing: inflow into the augmentor inlet, located on the upper surface of the delta wing, and entrainment into the plume of the augmentor exhaust. Simple models for both flow fields are proposed and integrated into the Brown and Michael cross-flow plane equilibrium formulation. The analysis suggests that serious lift penalties can be expected as a result of the interaction of augmentor-induces flow fields with the separated flow on the leeward side of a delta wing aircraft in transition.

CONTENTS

NOMENCLATURE

c	wing semi-span
C_μ	non-dimensional primary jet thrust
C_N	wing normal force coefficient
C_{Np}	wing normal force coefficient component due to jet entrainment
$F_p, F_i,$	
$F_v,$	complex velocity potentials for plume, inlet, vortex system
M	kinematic momentum flux
q	sink intensity
t	"inner" variable in free jet solution
T_o	augmentor primary jet thrust
w, ζ	complex representation of physical, transformed planes
u, v	x-,y-velocity components induced by viscous solution of 2-D turbulent free jet
x, y	coordinates in free jet/infinite wall plane, also real and imaginary coordinates in z-plane and w-plane.
z	complex plane in free jet/infinite wall analysis
V_∞	free-stream velocity
V_{fs}	cross-flow plane component of free-stream velocity
w_o, ζ_o	vortex location
α, ϵ	angle of attack, semi-apex angle
Γ	vortex intensity
ν, η	real and imaginary coordinates in ζ-plane
η_1, η_2	mappings of L,d in ζ-plane
ϕ	thrust augmentation coefficient
Φ	complex velocity potential in free jet/infinite wall analysis
ρ	ambient fluid density
σ	experimental constant in free jet equations

INTRODUCTION

In this simple analysis an attempt was made to assess the effects of operating a thrust augmentor installed on a delta wing aircraft during transition flight. The transition phase of a VSTOL aircraft occurs when the aircraft transfers from hover to horizontal flight. During this phase the aircraft derives its lift from aerodynamic forces and the direct thrust provided by the augmentors. This situation is schematically illustrated in Fig. 1.

A thin delta wing operates almost always in a regime of orderly separated flow on its leeward side. The separated vortical flow contributes substantially to the aerodynamic lift. When the thrust augmentor is activated, the flow fields induced by suction into the augmentor inlet and by entrainment into the exhaust jet plume interact with the separated vortical flow, affecting the aerodynamic lift. In addition to causing changes in the intensity and location of the vortical flow, the operation of the augmentor leads to decreased pressures in the neighborhood of the inlet on the upper surface due to inlet inflow, and in the lower surface of the wing due to entrainment-induced flow.

Drastic simplifications are required to extract any type of analytical information from such a complex aerodynamic problem. A number of delta-wing-related aerodynamic problems have been treated in the framework of the so-called cross-flow plane approach, first implemented by Brown and Michael[1]. Studies using this technique tend to predict the correct trends, such as the analysis of flapped delta wings by Oh et al[2]. Tavella[3] analyzed delta wings with lateral leading edge blowing and found remarkable agreement with experiments. From the analysis undertaken here it is expected that approximate trend will be extracted and appropriate combinations of non-dimensional parameters will be suggested.

MATHEMATICAL MODEL

Fig. 2 shows a cross-sectional cut of the idealized mathematical model. The wing is assumed to be flat. The separated vortical flow is simulated by a pair of concentrated vortices connected to the wing leading edges by feeding sheets. The conical augmentor is simulated by an inflow region of width 2d on the upper surface, and by a sink distribution beginning at a distance L below the wing and extending to $-\infty$ along the symmetry axis, representing entrainment. The entrainment into the exhaust jet is computed by assuming that the exhaust jet is two-dimensional, emanating from an infinitely thin slit, and discharging in quiescent air. To provide a distribution of entrainment, the jet is supposed to start at the lower surface, but the function representing the entrainment distribution is started at a distance L below the surface.

Conformal Transformation

The wing trace in the w-plane is transformed to a segment of the imaginary axis in the transformed ζ-plane by

$$w = \sqrt{\zeta^2 - 1} \tag{1}$$

as shown in Fig. 1 In the transformed plane the boundary conditions corresponding to the four basic components of the flow field, free-stream normal component, vortex, inlet and exhaust entrainment, are satisfied automatically.

Force due to Self-Similar 2-D Jet Exiting from a Wall Slit

The pressure acting on the lower surface of the wing is assessed by assuming that the exhaust jet can be simulated with a distribution of sinks that characterize entrainment. This is done by analyzing the flow field induced by a two-dimensional turbulent jet originating at an infinitely thin slot. For the purpose of this section, consider a jet originating at the origin of coordinates x,y, and having a symmetry axis coincident with the x-axis.

The velocity field of such a jet is given by[4]

$$u(x,y) = \sqrt{3/4}\sqrt{\frac{M\sigma}{x}}[1 - R(t)^2] \tag{2}$$

$$v(x,y) = \sqrt{3/16}\sqrt{\frac{M}{x\sigma}}\{2t[1 - R(t)] - R(t)^2\} \tag{3}$$

where

$$R(t) = \frac{1 - \exp(-2t)}{1 + \exp(-2t)} \tag{4}$$

with $t = \sigma y/x$ and $\sigma = 7.67$, an experimentally adjusted constant.
In these expressions t is an inner variable in an inner-outer matching sense. The sink distribution simulating entrainment is obtained by evaluating v(x,y) for $t \to \infty$. The sink intensity is of the form

$$q = q_o/\sqrt{x} \tag{5}$$

with

$$q_o = \sqrt{\frac{3M}{16\sigma}} \tag{6}$$

where M is the jet momentum flux divided by the jet density. An estimation of the nature of the force induced by the jet entrainment is obtained by integrating the pressure acting on an infinite wall. This is best done by placing the sink distribution in the imaginary plane and identifying the wall with the imaginary y-axis. The desired effect is achieved by reflecting the sink distribution about the origin of the real axis, as shown in Fig. 3. The velocity potential of this distribution is of the form

$$\Phi(z) = q_o/\pi\int_{-\infty}^{\infty}\frac{1}{\sqrt{|x|}}\ln(z - x)dx \tag{7}$$

The complex velocity is obtained by differentiating Eq. 7 with respect to z within the integral. The velocity at the wall results from setting $z = iy$ and rewriting the integral in the interval $-\infty$ to ∞ as follows

$$v(iy) = 2q_o/\pi \int_0^\infty \frac{y}{\sqrt{x}\,(x + iy)(x - iy)} dx \tag{8}$$

This integral can be performed exactly by residues. There results

$$v_{wall} = -q_o \sqrt{\frac{2}{y}} \tag{9}$$

Since the pressure acting on the wall is proportional to the square of the velocity, the integral of the pressure over the entire wall is divergent. To avoid this difficulty, the distribution of entrainment is assumed to start at a distance L below the wing surface, as illustrated in Fig. 2.

Complex Potential for the Plume

The effect of the plume is represented by a sink distribution which maps according to

$$|q(\zeta)| = |q(w)| \left|\frac{dw}{d\zeta}\right| \tag{10}$$

The sink distribution in the physical plane is given by

$$|q(w)| = \frac{q_o}{|\sqrt{w}|} \tag{11}$$

Substituting for w

$$|q(w)| = \frac{q_o}{|(\zeta^2 + 1)^{1/4}|} \left|\frac{\zeta}{\sqrt{(\zeta^2 + 1)}}\right| \tag{12}$$

With $\zeta = i\eta$, $\eta < -\eta_1$, where $i\eta_1$ is the mapping in the transformed plane of $w = iL$, Eq. (12) can be rewritten

$$|q(w)| = q_o \exp(-i\pi/4) \frac{\zeta}{(\zeta^2 + 1)^{3/4}} \tag{13}$$

An integral involving $|q(w)|$ is required to compute the velocity potential due to the presence of the plume. The expression given by Eq. (13) is not integrable in closed form, instead, an approximate composite expansion will be used, given by

$$|q(\zeta)| \simeq q_o \exp(-i\pi/4)\left[\frac{\exp(-i\pi/8)}{2^{3/4}(\zeta + i)^{3/4}} + \frac{1}{\sqrt{\zeta}} - \frac{\exp(-i\pi p/8)}{2^{3/4}(\zeta + i/2)^{3/4}}\right] \qquad (14)$$

The complex potential for the plume in the transformed plane is

$$F_p(\zeta) = \frac{1}{\pi}\int_{-i\infty}^{-i\eta_1} |q(\bar{\zeta})| \ln(\zeta - \bar{\zeta}) |d\bar{\zeta}| \qquad (15)$$

Setting the integration path $|d\bar{\zeta}| = id\zeta$, Eq. (15) becomes

$$F_p(\zeta) = \frac{i}{\pi}\int_{-i\infty}^{-i\eta_1} |q(\bar{\zeta})| \ln(\zeta - \bar{\zeta}) d\bar{\zeta} \qquad (16)$$

Using expression in Eq. (14) this integral can be carried out exactly. The complex potential due to entrainment into the plume is then

$$\begin{aligned} F_p(\zeta) = \frac{q_o}{\pi}\Bigg[\frac{4\exp(i\pi/8)}{2^{2/3}}\Bigg[2(\zeta + i)^{1/4}\left[\arctan\left(\frac{(\zeta + i)^{1/4}}{[i(\eta_1 + 1)]^{1/4}}\right)\right. \\ \left. + i\arctan\left(\frac{i(\zeta + i)^{1/4}}{[i(\eta_1 + 1)]^{1/4}}\right)\right] - [i(\zeta + 1)]^{1/4}[\ln(\zeta - i\zeta) - 4] \\ - 2(\zeta + i/2)^{1/4}\left[\arctan\left(\frac{(\zeta + i/2)^{1/4}}{[i(\zeta + 1/2)]^{1/4}}\right) + i\arctan\left(\frac{i(\zeta + i/2)^{1/4}}{[i(\zeta + 1/2)]^{1/4}}\right)\right] \\ + [i(\zeta + 1/2)]^{1/4}[\ln(\zeta - i\eta_1) - 4]\Bigg] + 2\exp(i\pi/4)\Bigg[i2\sqrt{\zeta}\arctan\left(\frac{i\sqrt{\zeta}}{\sqrt{i\eta_1}}\right) \\ - \sqrt{i\eta_1}[\ln(\zeta - i\eta_1) - 2]\Bigg]\Bigg] \end{aligned} \qquad (17)$$

Complex Potential for the Augmentor Inlet

In the transformed plane, the complex potential of the source distribution

representing the effect of the augmentor inlet can be written as

$$F_i(\zeta) = \frac{1}{\pi}\int_{\eta_2}^{i} q(\tau)\ln(\zeta - \tau)|d\tau| \tag{18}$$

where η_2 is the mapping of w = d in the transformed plane, as shown in Fig. 3. The source intensity is found from the expression

$$q(\zeta) = q_o\left|\frac{dw}{d\zeta}\right| \tag{19}$$

where q_o is the velocity at the augmentor inlet plane, which in this analysis is assumed to be constant. This velocity is related to the momentum of the exhaust jet and the thrust augmentation coefficient, the details can be found in the work by Lund et al[5]. The magnitude of the differential is found from the relationship

$$d\tau = |d\tau|\exp(i\pi/2) \tag{20}$$

Replacing in Eq. (18)

$$F_i(\zeta) = \frac{q_o}{\sqrt{2\pi}}\exp(i\pi/4)\int_i^{\eta_2}\frac{1}{\sqrt{(\tau - i)}}\ln(\zeta - \tau)d\tau \tag{21}$$

Performing this integral, the complex velocity is

$$\frac{dF_i}{d\zeta} = -i\sqrt{2}q_o\frac{\exp(i\pi/4)}{\sqrt{(\zeta - 1)}}\left[\arctan\left(\frac{i\sqrt{(\zeta - 1)}}{\sqrt{(\eta_2 - 1)}}\right) + \frac{\pi}{2}\right] \tag{22}$$

Transformation given by Eq. (1) can be expanded for small w

$$\zeta \simeq i(1 - \frac{1}{2}w^2) \tag{23}$$

Substituting for the mapping of η_2, Eq. (26) can be rewritten

$$\frac{dF_i}{d\zeta} = -i\sqrt{2}q_o \frac{\exp(i\pi/4)}{\sqrt{(\zeta - 1)}}\left[\arctan\left[\frac{i\sqrt{2}(\zeta - 1)}{\sqrt{-i(d/c)}}\right] + \frac{\pi}{2}\right] \tag{24}$$

Conical Kutta Condition

The Kutta condition requires that the velocity be finite at the edge of the delta wing. This requirement translates into a stagnation point at the origin in the transformed plane. Since the velocity is the sum of the contributions by the free-stream, the vortices, the inlet flow, and the flow induced by the plume entrainment, the Kutta condition establishes

$$iV_\infty\alpha - \frac{dF}{d\zeta}v(0) - \frac{dF}{d\zeta}i(0) - \frac{dF}{d\zeta}p(0) = 0 \tag{25}$$

Introducing a non-dimensional form of the primary jet thrust

$$C_\mu = \frac{T_o}{1/2\rho V_\infty^2 2c} \tag{26}$$

and the following parameter

$$K = \frac{\sqrt{\frac{(\phi - 1)}{d/c}\frac{C_\mu}{\epsilon^2}}}{\alpha/\epsilon} \tag{27}$$

after substitutions from Eqs. (17), (22), and the expression for the velocity due to the vortex system[1] in Eq. (25), an explicit relationship for the

vortex intensity can be obtained.

$$\frac{\Gamma}{2\pi V_\infty \alpha} = \frac{1 + \frac{K}{\pi} G(\sigma, d/c, L/c)}{\frac{\zeta_o + \bar{\zeta}_o}{\zeta_o \bar{\zeta}_o}} \tag{28}$$

where $G(\sigma, d/c, L/c)$ is a very complicated complex function that in this work was computed numerically in the process of solving the singularities equilibrium problem.

Vortex Equilibrium Position

The equilibrium position of the vortex system is found by requiring that the net forces acting on the vortices be balanced by the forces acting on the connecting sheets. The velocity due to the vortices is singular at the vortices cores locations. A limit process is required to obtain a finite value at the core. This is done in a manner similar to Brown and Michael[1]. The complex velocity due to the vortex system at the core location is

$$\frac{dF_v}{dw} = \frac{i\Gamma}{2\pi}\left[\frac{w_o}{(w_o^2 - 1) + \sqrt{((w_o^2 - 1)(\bar{w}_o^2 - 1))}} + \frac{1}{2}\frac{1}{w_o(w_o^2 - 1)}\right] \tag{29}$$

With the definitions

$$V_v = \frac{dF_v}{dw} \tag{30}$$

$$V_i = \frac{dF_i}{dw} \tag{31}$$

$$V_p = \frac{dF_p}{dw} \tag{32}$$

the complex velocity in the cross flow plane can be expressed

$$\frac{dF}{d\zeta} = V_\infty \alpha\left[\frac{\Gamma}{2\pi V_\infty \alpha} - i + K(V_i + V_p)\right] \tag{33}$$

The equation expressing force balance, to be solved for the vortex position w_o is

$$\frac{\alpha}{\epsilon}\frac{\Gamma}{2\pi V_\infty \alpha}V_v(\zeta(w_o)) + \frac{\alpha}{\epsilon}\frac{w_o}{\sqrt{(w_o - 1)}\sqrt{(w_o + 1)}}\Big[V_{fs}(\zeta(w_o)) + K\Big[V_i(\zeta(w_o)) + V_p(\zeta(w_o))\Big]\Big] = (2\bar{w}_o - 1) \qquad (34)$$

This equation is solved for the vortex position by iteration. Once the vortex position is known, the vortex intensity is computed from Eq. (28).

Normal Force Coefficient

The normal force exerted on the wing is computed by considering the vertical momentum flux through a plane normal to the wing surface. The same process as indicated in [1] is followed. The aerodynamic component of such force, which excludes the direct thrust of the augmentor, is

$$\frac{C_N}{\epsilon^2} = 2\pi\frac{\alpha}{\epsilon} + 8\pi\frac{\Gamma}{2\pi V_\infty \alpha}\mathrm{Re}(\zeta_o/c)\frac{\alpha}{\epsilon} + 2\sqrt{(\phi - 1)\frac{C_\mu}{\epsilon^2}\frac{d}{c}}\frac{\alpha}{\epsilon} + (\phi - 1)\frac{C_\mu}{\epsilon^2} + 4\sqrt{(\phi - 1)\frac{C_\mu}{\epsilon^2}\frac{d}{c}} + C_{Np} \qquad (35)$$

where ϕ is the augmentor thrust augmentation. The normal force coefficient appears as the sum of six terms. The first term represents the linear component of lift that would occur in the absence of the augmentor and if the flow field were attached. The second term represents the vortical lift. The third and fifth terms represent the effect of changing scales of the cross-flow motion associated with the augmentor presence. The fourth term represents the suction related to inlet inflow, acting on the upper wing surface. The last term indicates the contribution from suction due to entrainment into the exhaust plume, acting on the lower surface. No closed form was found for this contribution.

RESULTS AND DISCUSSION

Fig. 4 summarizes the effect of augmentor operation on normal force coefficient. In these figures basic lift is the normal force coefficient that would occur in the absence of the augmentor. Aerodynamic lift is the normal force coefficient that would result from the integration of the surface pressure acting on the wing in the presence of the augmentor. The total lift is the aerodynamic lift plus the direct thrust of the augmentor. In all cases, when the augmentor is activated, a minimum value of α/ϵ exists below which no solution for an equilibrium vortex position can be found. The following trends can be observed:

a) The effect of operating the augmentor is a marked reduction of the aerodynamic lift. In many cases this reduction is offset almost exactly by the direct thrust of the augmentor.

b) The negative impact of augmentor flow interaction on lift is more pronounced at low direct thrust, low thrust augmentation and higher angle of attack.

c) A wider augmentor inlet width is slightly more favorable than a narrower one. This is a surprising result, since a narrow inlet width would tend to produce a concentration of negative pressure, whose integration on the upper surface is expected to diverge as the inlet width vanishes.

d) The effect of where the entrainment into the exhaust jet is allowed to begin is very small on global lift, for $L/c > 0.2$. As L vanishes, however, the lift is expected to be totally upset by suction forces on the lower surface.

e) The computations indicate that to avoid dramatic lift losses the augmentation ratio should be of order 1.8.

CONCLUSIONS

In the framework of the idealized analysis presented here, it is found that the operation of a conical augmentor integrated into a delta wing may, under most circumstances, lead to little or no net lift augmentation. In many instances drastic lift reduction is expected. The negative effects are significantly ameliorated only at unreasonably high thrust augmentations (1.8 or more.) It is also predicted that these negative effects will be less pernicious at the stage of transition flight when augmentor operation is needed the most. This situation would occur at the early part of transition, when the non-dimensional augmentor thrust, C_μ, is large.

Due to the extreme idealizations imbedded in this analysis, primarily the assumption that the entrainment into the exhaust is unaffected by the longitudinal free-stream velocity component, the trends revealed by the results are only to be taken as a preliminary warning of what might happen in a more realistic context.

REFERENCES

1. Brown, C.E. and Michael, W.H. Jr., "On Slender Delta Wings with Leading Edge Separation," NACA TN 3430, March 1955.

2. Oh, Sejong and Tavella, D., "Analysis of a Delta Wing with Leading Edge Flaps," J. of Aircraft, Vol. 24, No. 6, June 1987.

3. Tavella, D., "Lift of Delta Wings with Leading Edge Blowing," to appear in J. of Aircraft, March 1988.

4. Schlichting, H., Grenzschicht Theorie, Verlag G. Braun, Karlsruhe, 1964.

5. Lund, T.S., Tavella, D.A. and Roberts, L., "A Computational Study of Thrust Augmenting Ejectors Based on a Viscous-Inviscid Approach," JIAA TR 77, Stanford University, May 1987.

FIGURES

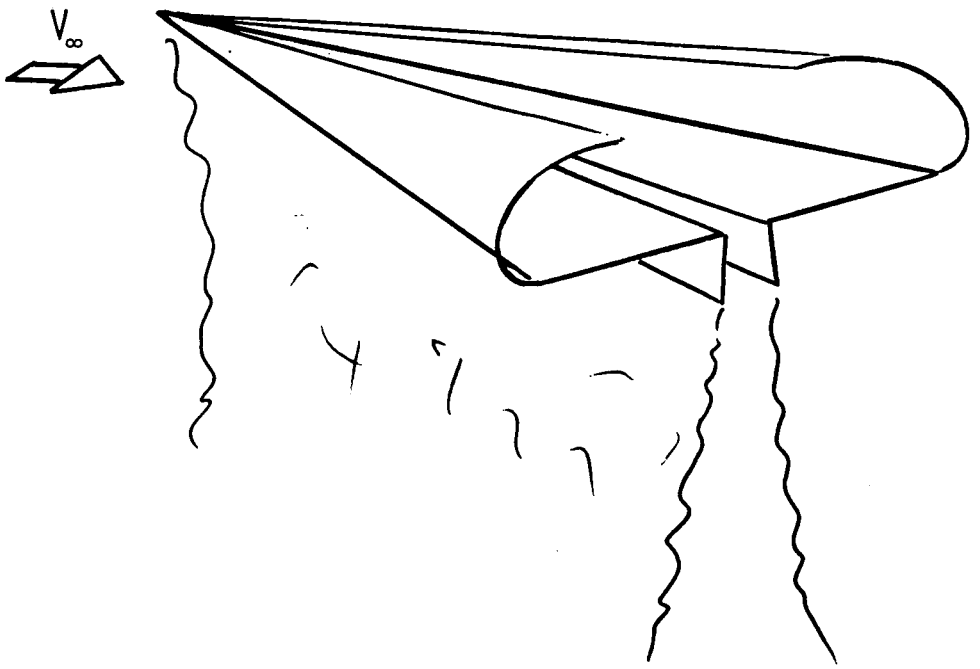

Figure 1. Conical augmentor/delta wing

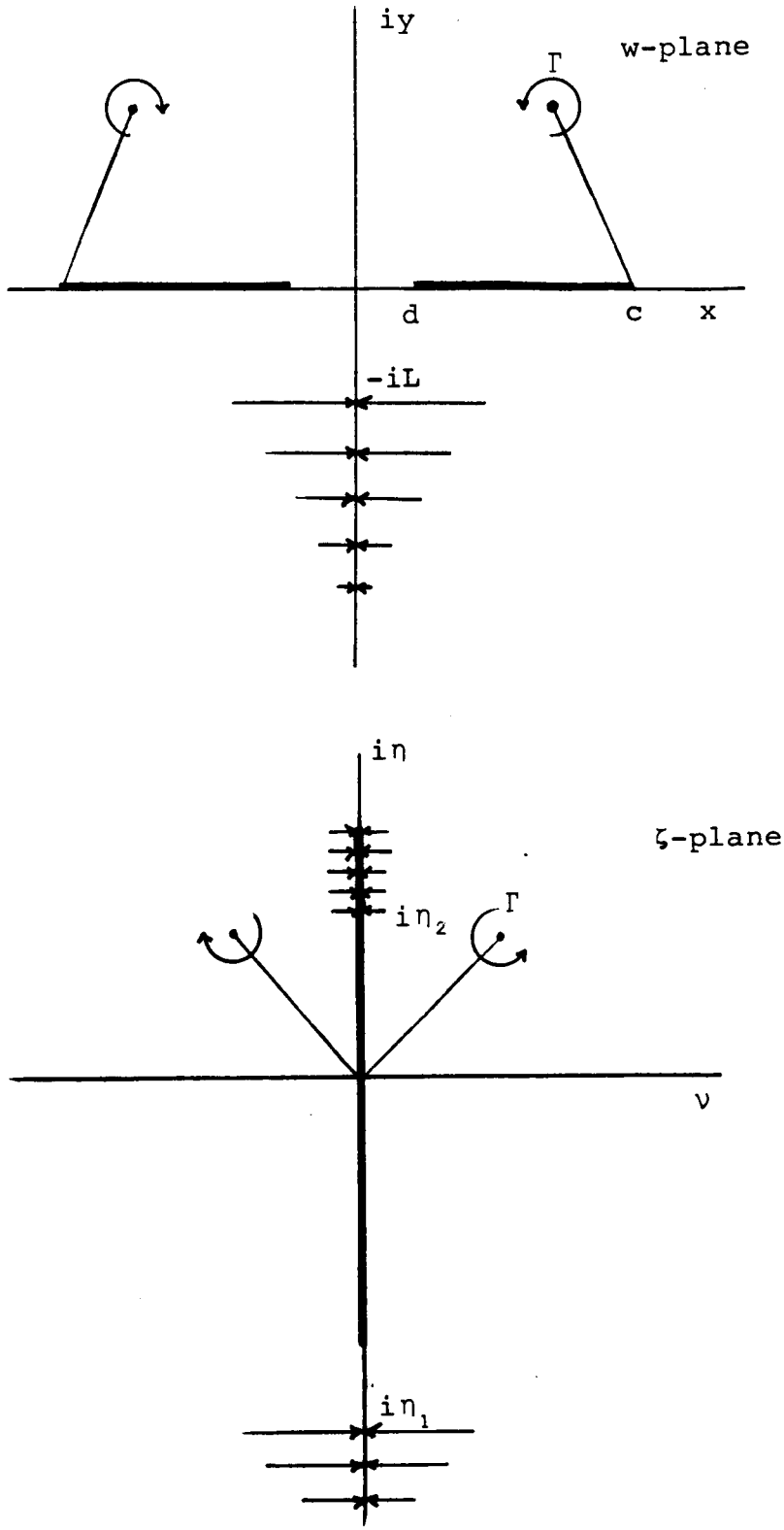

Figure 2. Mathematical model and wing trace

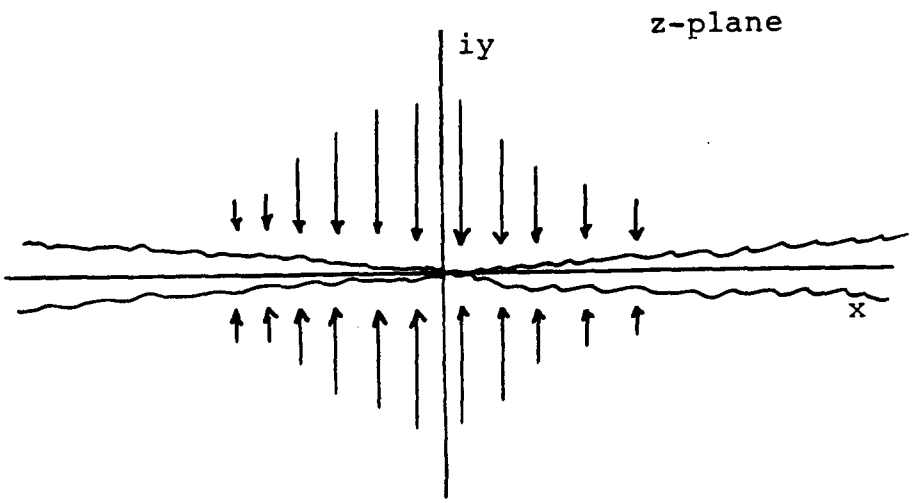

Figure 3. Plane jet from wall slit

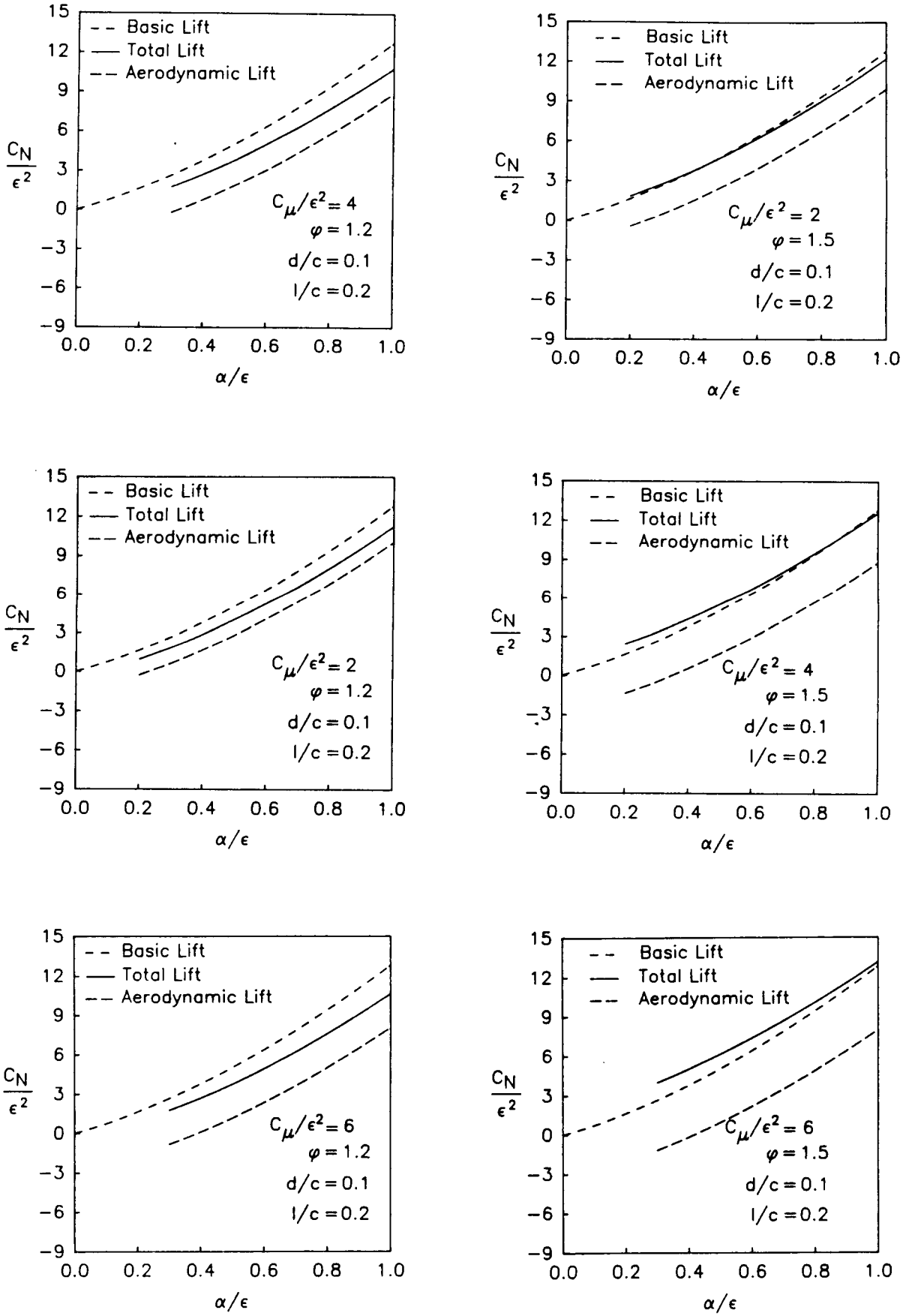

Figure 4. Augmentor integration performance

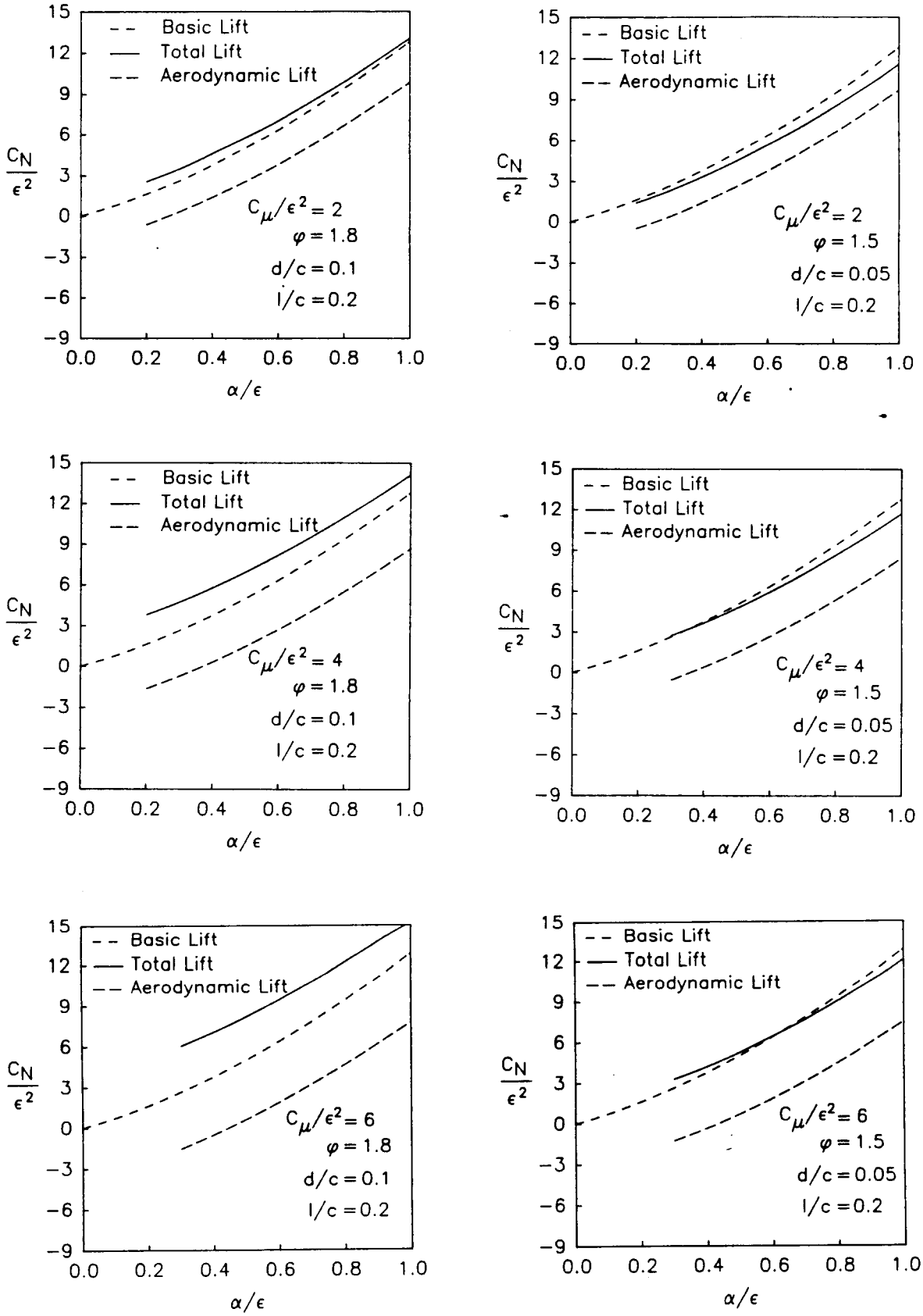

Figure 4. Continued

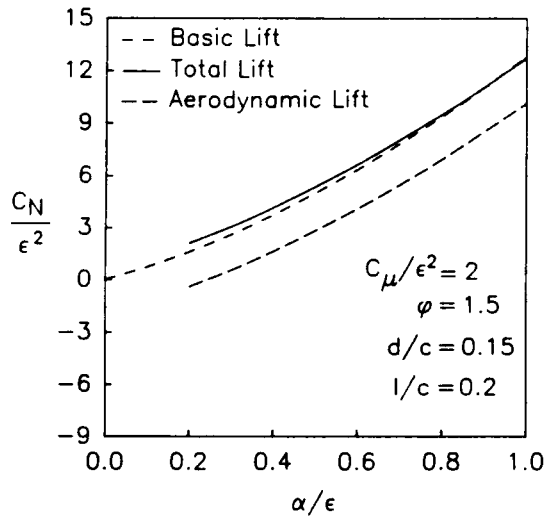

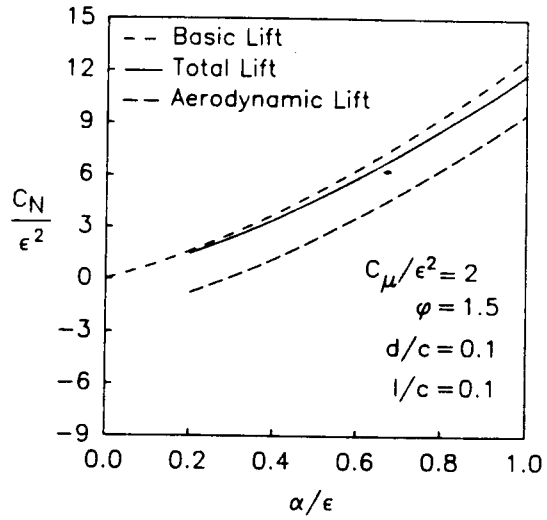

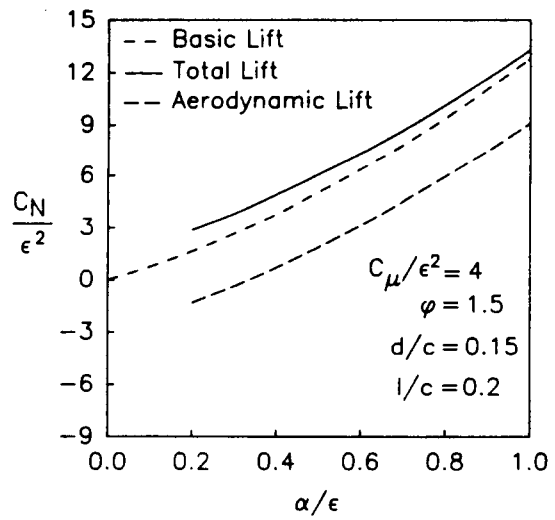

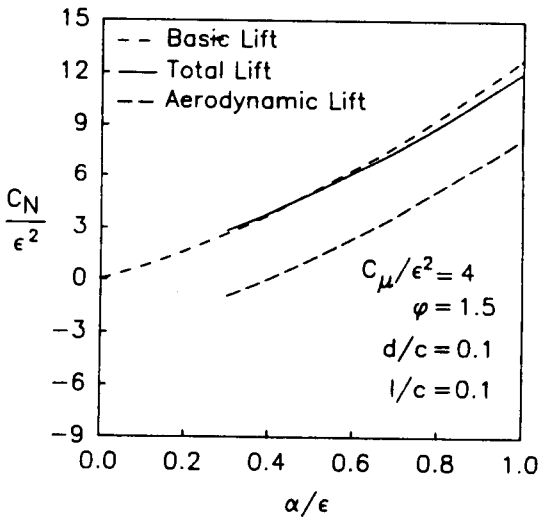

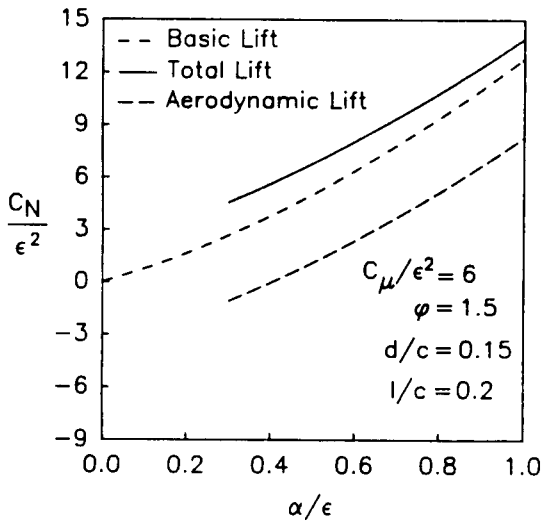

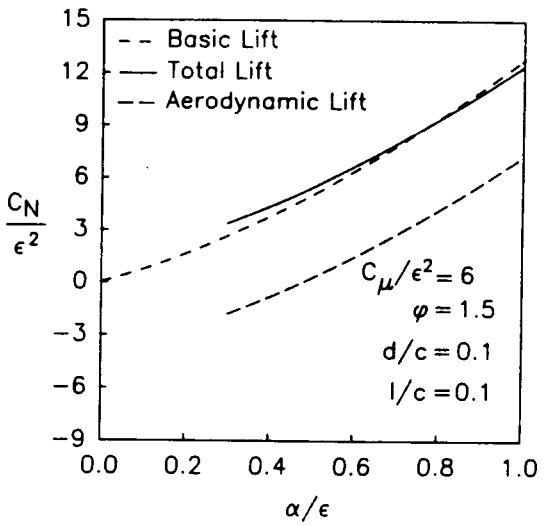

Figure 4. Continued

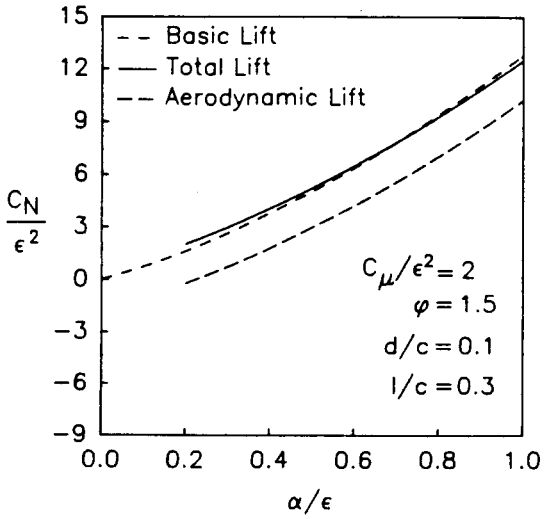

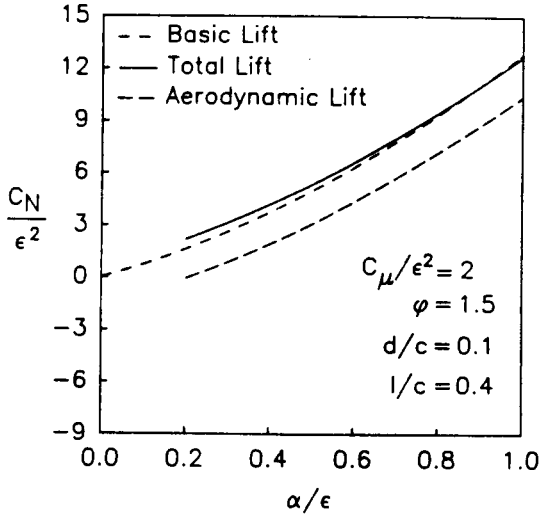

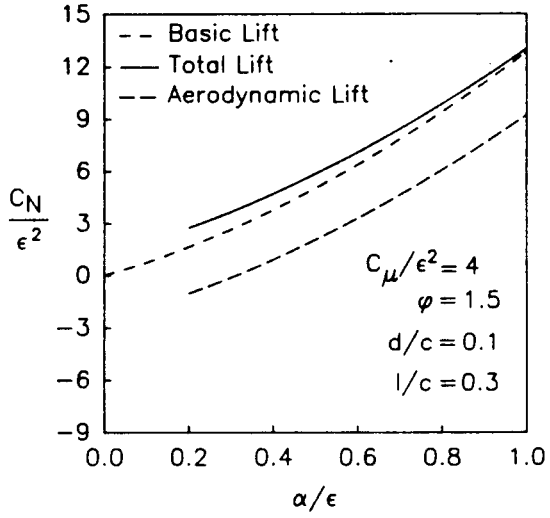

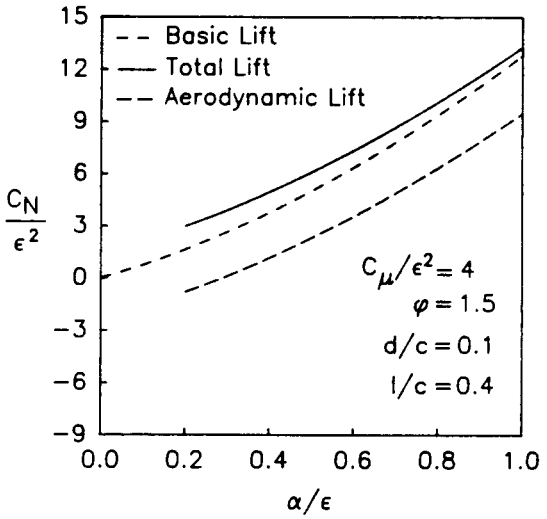

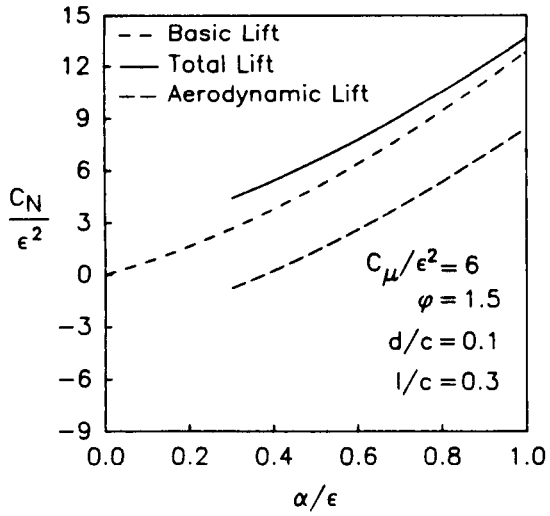

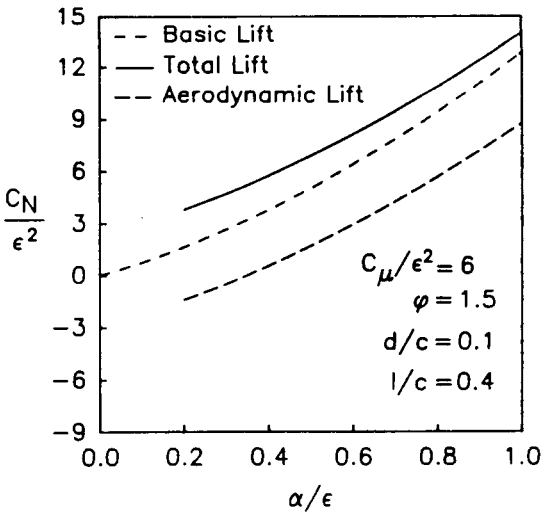

Figure 4. Continued